Supplement of

Modeling seismic site response to improve lacustrine paleoseismic records

Yang et al.

Correspondence to: Huitong Yang (Huitong.Yang@UGent.be)

Introduction

The supplementary material for this manuscript contains additional figures and tables that support the main text.

Figures S1 presents the geometry of the 2D flat-layer models (FM01 and FM02) used for reference site response simulations.

Figures S2 and S3 show along-profile PGA and PGV results from the 2D basin model using the alternative V_p model with unconsolidated glaciolacustrine deposits setting.

Figure S4 provides detailed medical CT images of sediment cores from Lake Riñihue, illustrating stratigraphic correlation across the 1960 CE earthquake horizon and the classification of soft-sediment deformation structures.

Figures S5–S8 present the PGA and PGV results from the flat-layer model simulations (FM01 and FM02) under different units' parameters.

Figures S9 and S10 show multivariate regression results relating SSR depth to slope angle and ground motion parameters (PGA and PGV, respectively) from both GMPE predictions and 2D simulations.

Figures S11–S13 present the univariate and multivariate regression analyses for SSDS thickness.

Table S1 show parameters for the 2D numerical modeling using the alternative V_p model with unconsolidated glaciolacustrine deposits setting.

Table S2 list the detailed material properties assigned to the flat-layer and basin models.

Table S3 compiles the full set of regression equations and R^2 values for all SSR and SSDS models tested.

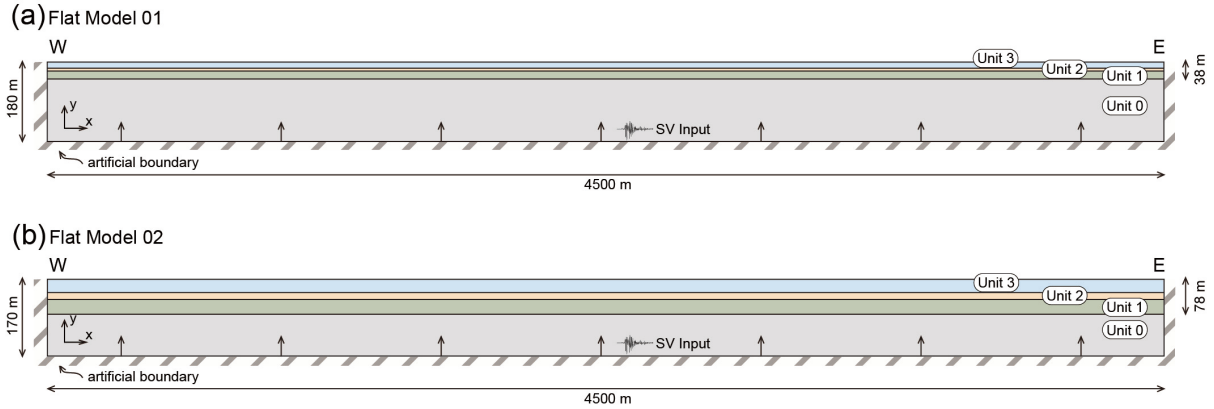

Figure S1. Sketch map of the 2D flat-layer models used for site response simulations. (a) FM01 with total depth of 180 m and sediment thickness of 38 m, corresponding to the western central of the basin profile. (b) FM02 with total depth of 170 m and sediment thickness of 78 m, corresponding to the eastern central basin. These models correspond to the reference locations indicated by red arrows in Figure 3. Both models are 4500 m wide and include four units (Units 0–3) with the same properties setting as the 2D basin model (Table 2, Table S2). Absorbing boundaries are applied at the base and lateral edges. SV-wave input is applied from the base.

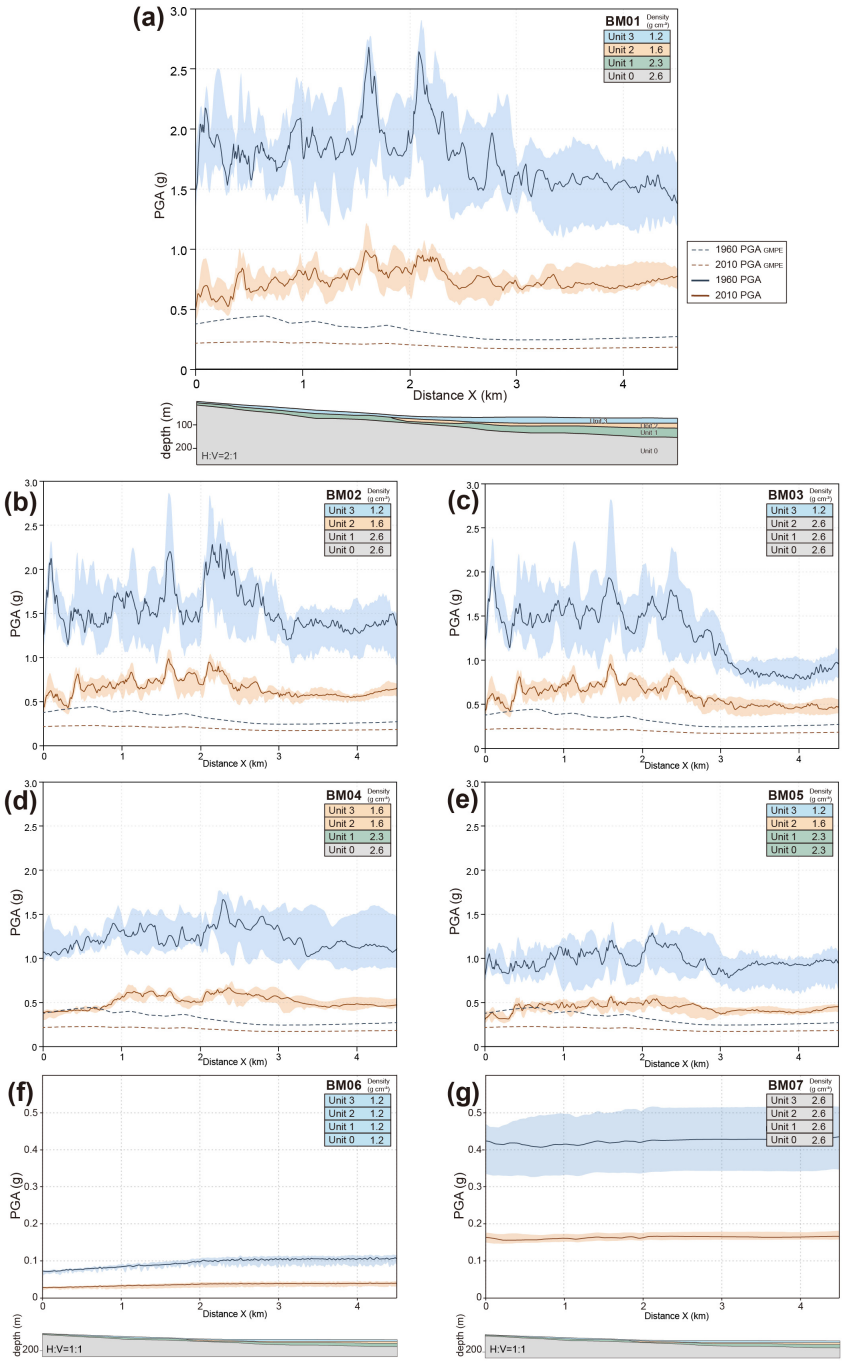

Figure S2. Along-profile PGA from 2D numerical simulations using the alternative V_P model (Vp = 1800 m/s for glaciolacustrine deposits; Table S1) for seven set of basin model parameters (Table 2). Layout and symbols follow Figure 6. (a) BM01 with realistic stratigraphy. (b–e) Models with progressively modified unit properties. (f–g) Uniform end-member models. Solid lines show median PGA for the 1960 (blue) and 2010 (orange) earthquakes; shaded envelopes span the range across seven input motions. Dashed lines in (a) indicate GMPE predictions. Depth-converted cross-sections are shown beneath (a), (f), and (g).

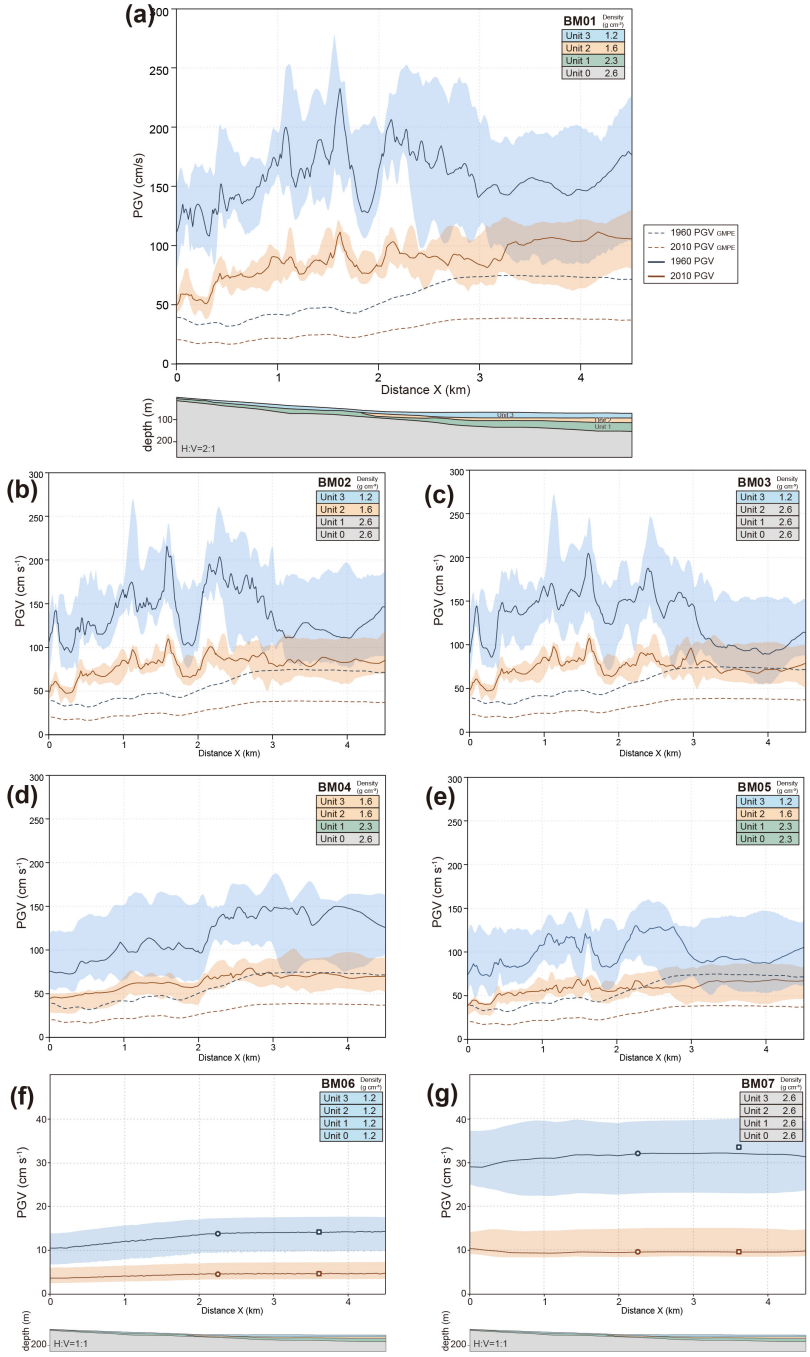

Figure S3. Along-profile PGV from 2D numerical simulations using the alternative V_P model (Vp = 1800 m/s for glaciolacustrine deposits; Table S1) for seven set of basin model parameters (Table 2). Layout and symbols follow Figure 7. (a) BM01 with realistic stratigraphy. (b–e) Models with progressively modified unit properties. (f–g) Uniform end-member models. Solid lines show median PGV for the 1960 (blue) and 2010 (orange) earthquakes; shaded envelopes span the range across seven input motions. Dashed lines in (a) indicate GMPE predictions. Depth-converted cross-sections are shown beneath (a), (f), and (g).

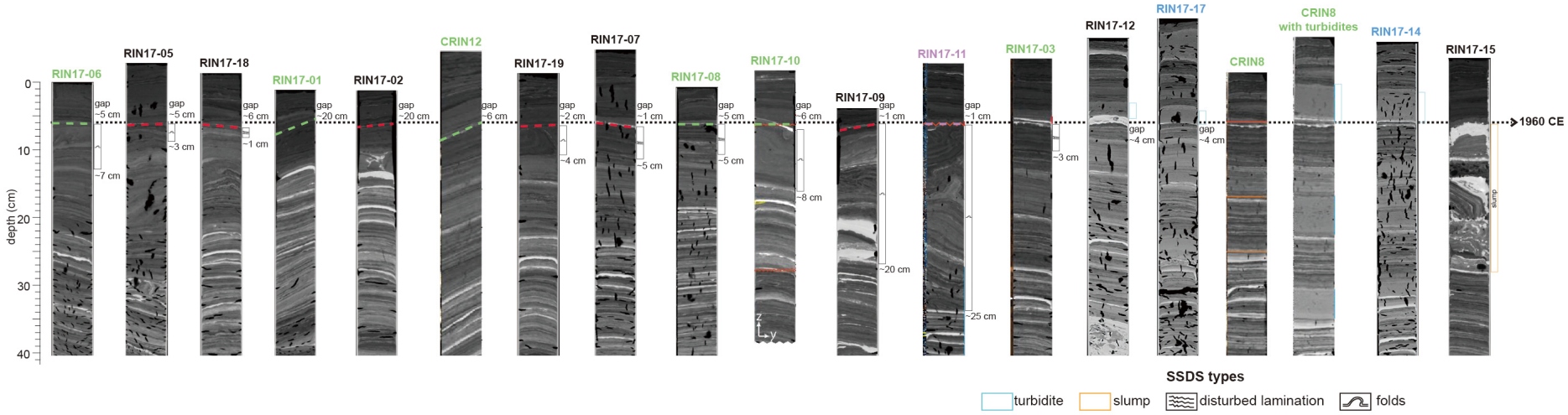

Figure S4. Medical CT scan images from Lake Riñihue showing stratigraphic correlation across the 1960 CE earthquake horizon (dashed black line). Core names in green (e.g., RIN17-06) are adapted from Molenaar et al. (2021), in purple (e.g., RIN17-11) are adapted from Molenaar et al. (2022), black labels (e.g., RIN17-05) indicate slope cores and blue labels (e.g., RIN17-17) indicate cores from the flat interior basin analyzed in this study. Colored dashed lines show where the gaps are caused by surficial remobilization, with estimated remobilization depth. SSDS types according to legend are shown with its thickness. Core locations shown in Figure 1b.

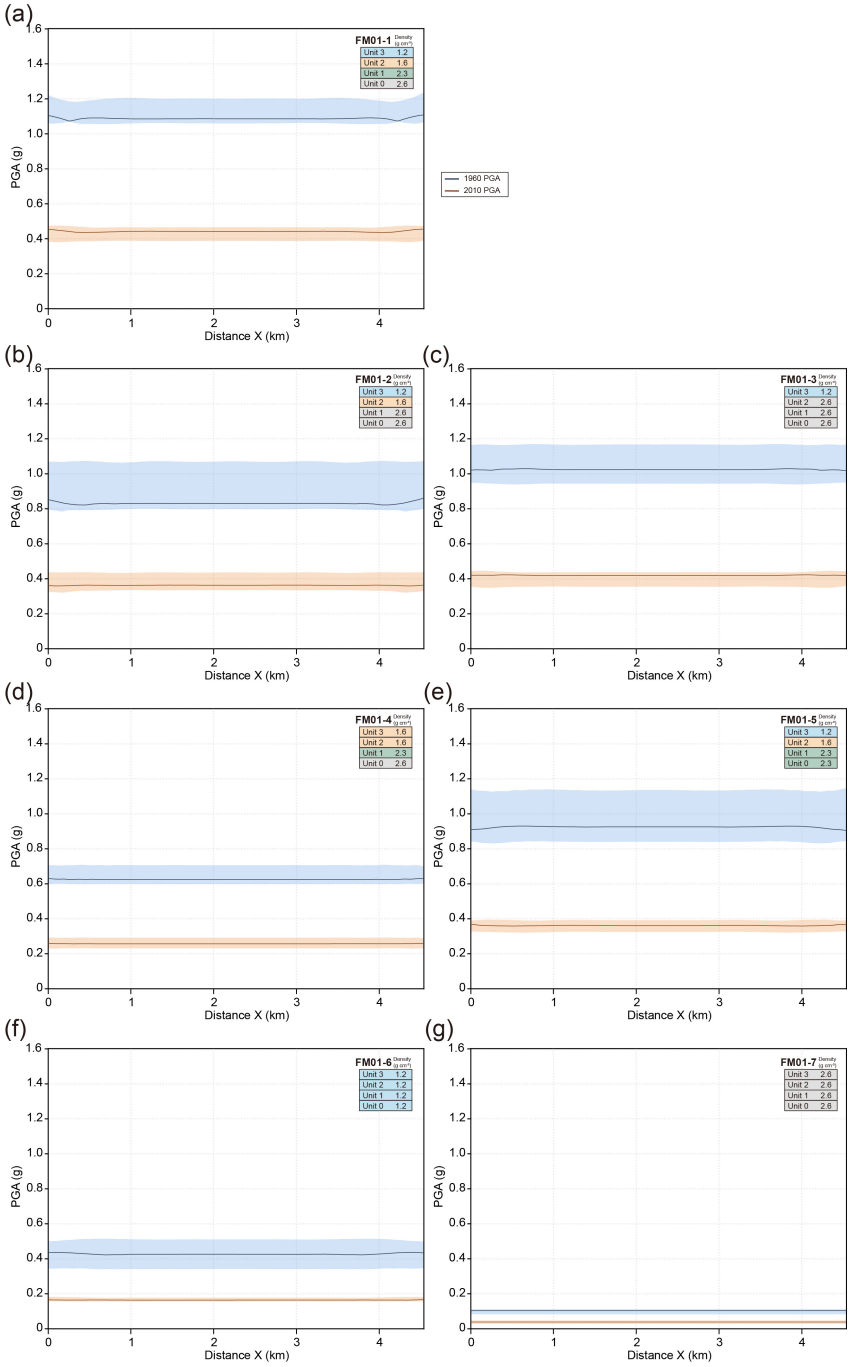

Figure S5. Along-profile peak ground acceleration (PGA) from2D numerical simulations using FM01 structure for seven set of unit parameters (Table 2, Table S1). (a) FM01-1 with original stratigraphy. (b–e) FM01-2 to FM01-5 with gradually replacement of deeper units with stiffer properties. (f–g) Uniform end-member FM01-6 and FM01-7 with Holocene and bedrock properties, respectively. Blue and orange lines represent calculated mean PGA for the 1960 and 2010 earthquakes, respectively; shaded areas show the results range across seven input motions.

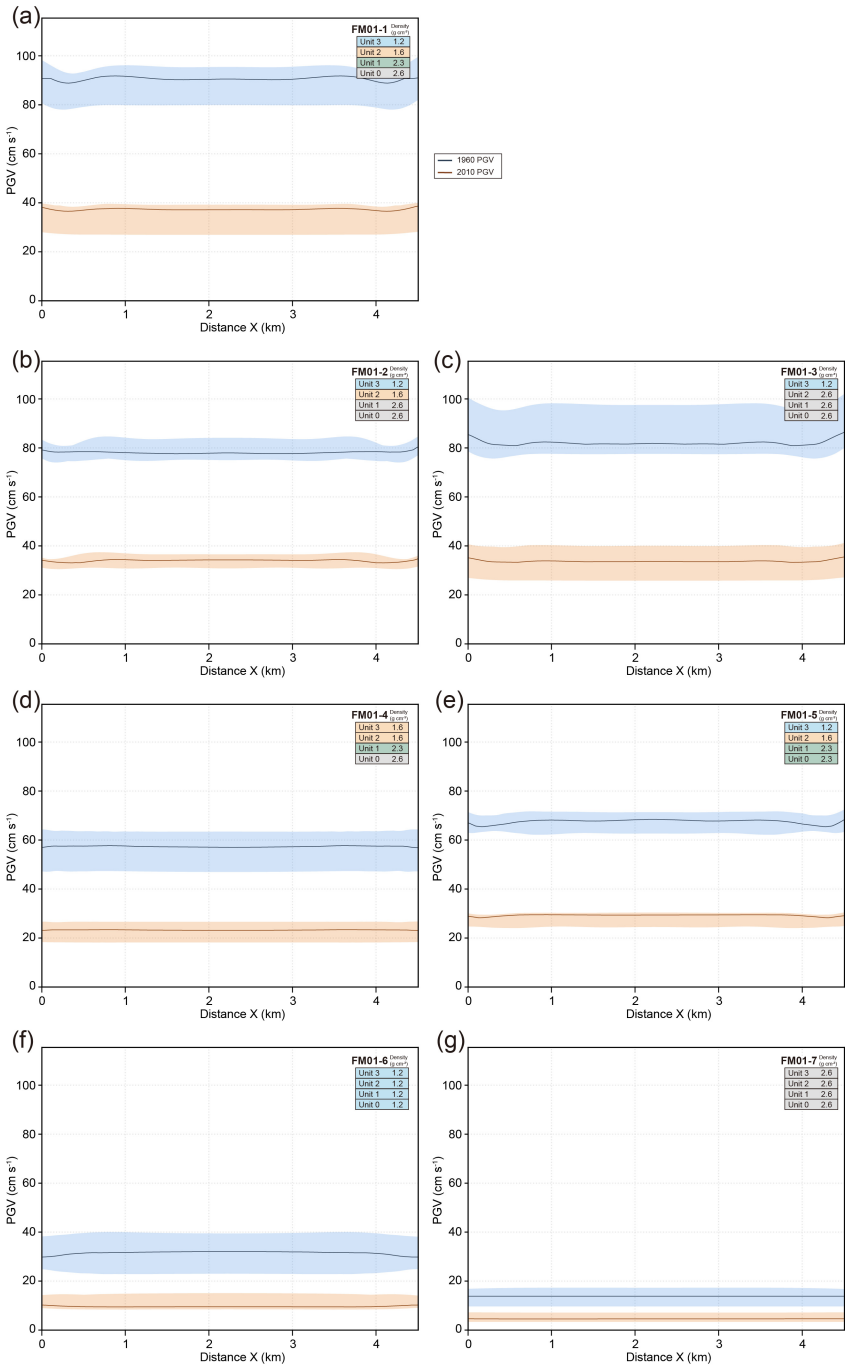

Figure S6. Along-profile PGV from2D numerical simulations using FM01 structure for seven set of unit parameters (Table 2, Table S1). (a) FM01-1 with original stratigraphy. (b–e) FM01-2 to FM01-5 with gradually replacement of deeper units with stiffer properties. (f–g) Uniform end-member FM01-6 and FM01-7 with Holocene and bedrock properties, respectively. Blue and orange lines represent calculated mean PGV for the 1960 and 2010 earthquakes, respectively; shaded areas show the results range across seven input motions.

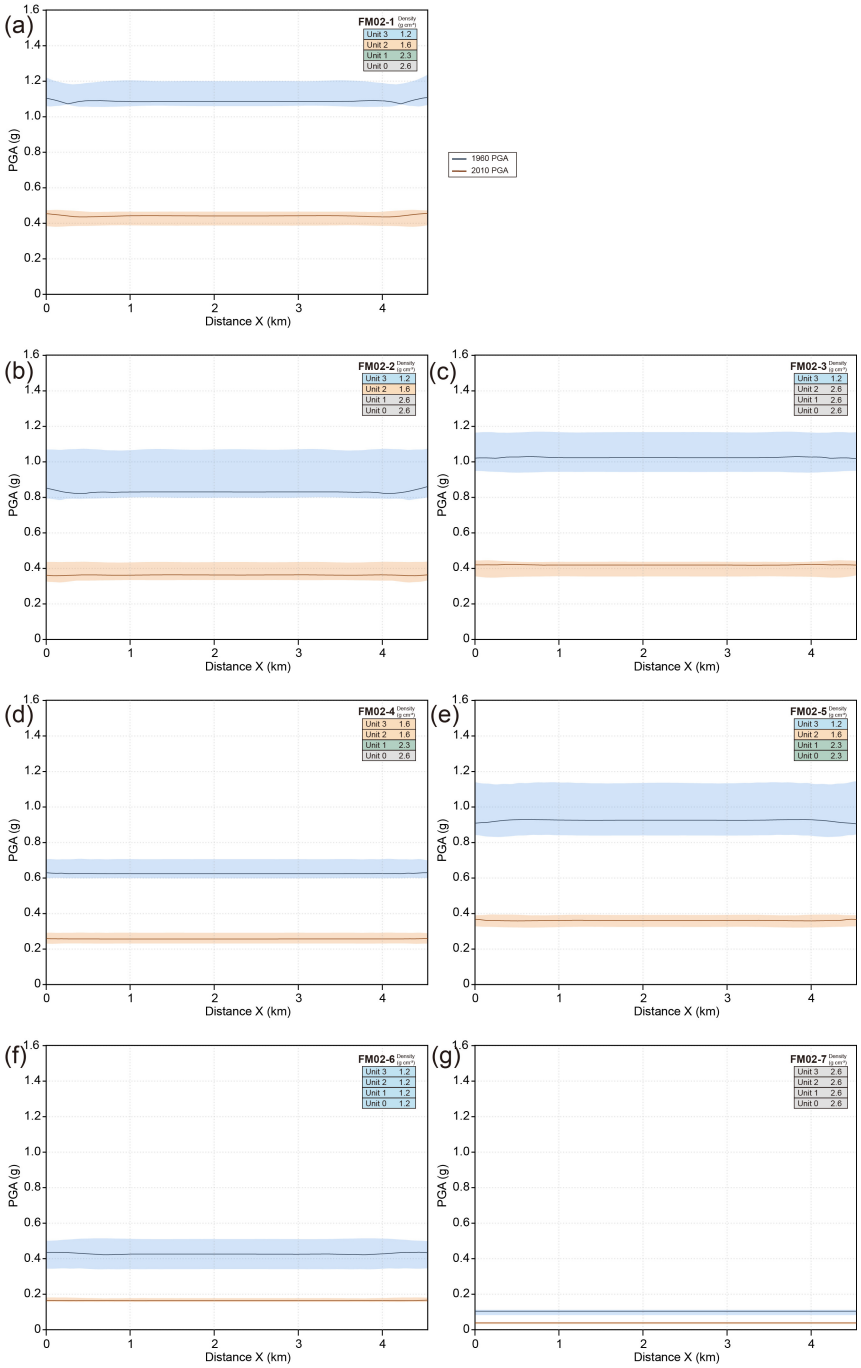

Figure S7. Along-profile peak ground acceleration (PGA) from2D numerical simulations using FM02 structure for seven set of unit parameters (Table 2, Table S1). (a) FM02-1 with original stratigraphy. (b–e) FM02-2 to FM02-5 with gradually replacement of deeper units with stiffer properties. (f–g) Uniform end-member FM02-6 and FM02-7 with Holocene and bedrock properties, respectively. Blue and orange lines represent calculated mean PGA for the 1960 and 2010 earthquakes, respectively; shaded areas show the results range across seven input motions.

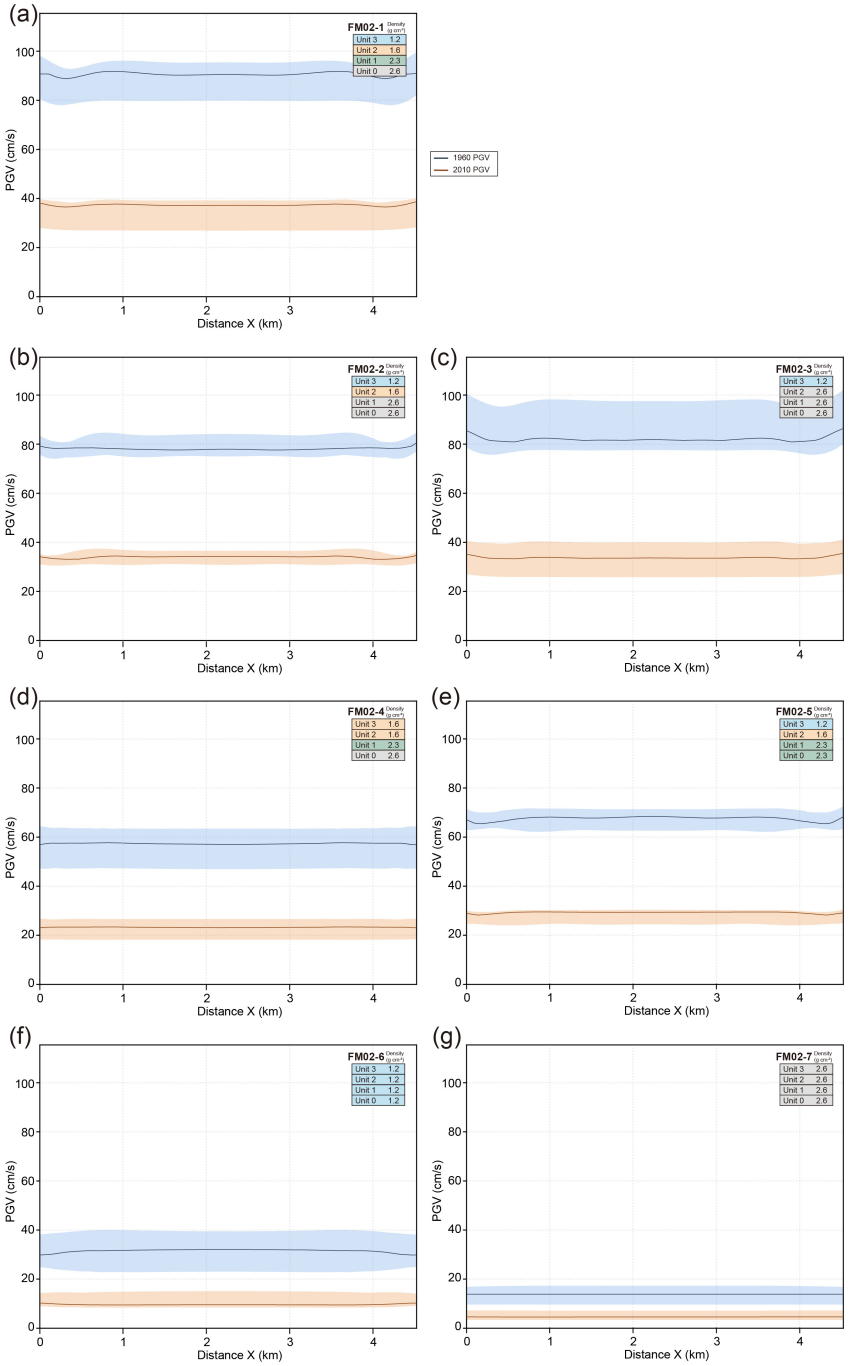

Figure S8. Along-profile PGV from2D numerical simulations using FM02 structure for seven set of unit parameters (Table 2, Table S1). (a) FM02-1 with original stratigraphy. (b–e) FM02-2 to FM02-5 with gradually replacement of deeper units with stiffer properties. (f–g) Uniform end-member FM02-6 and FM02-7 with Holocene and bedrock properties, respectively. Blue and orange lines represent calculated mean PGV for the 1960 and 2010 earthquakes, respectively; shaded areas show the results range across seven input motions.

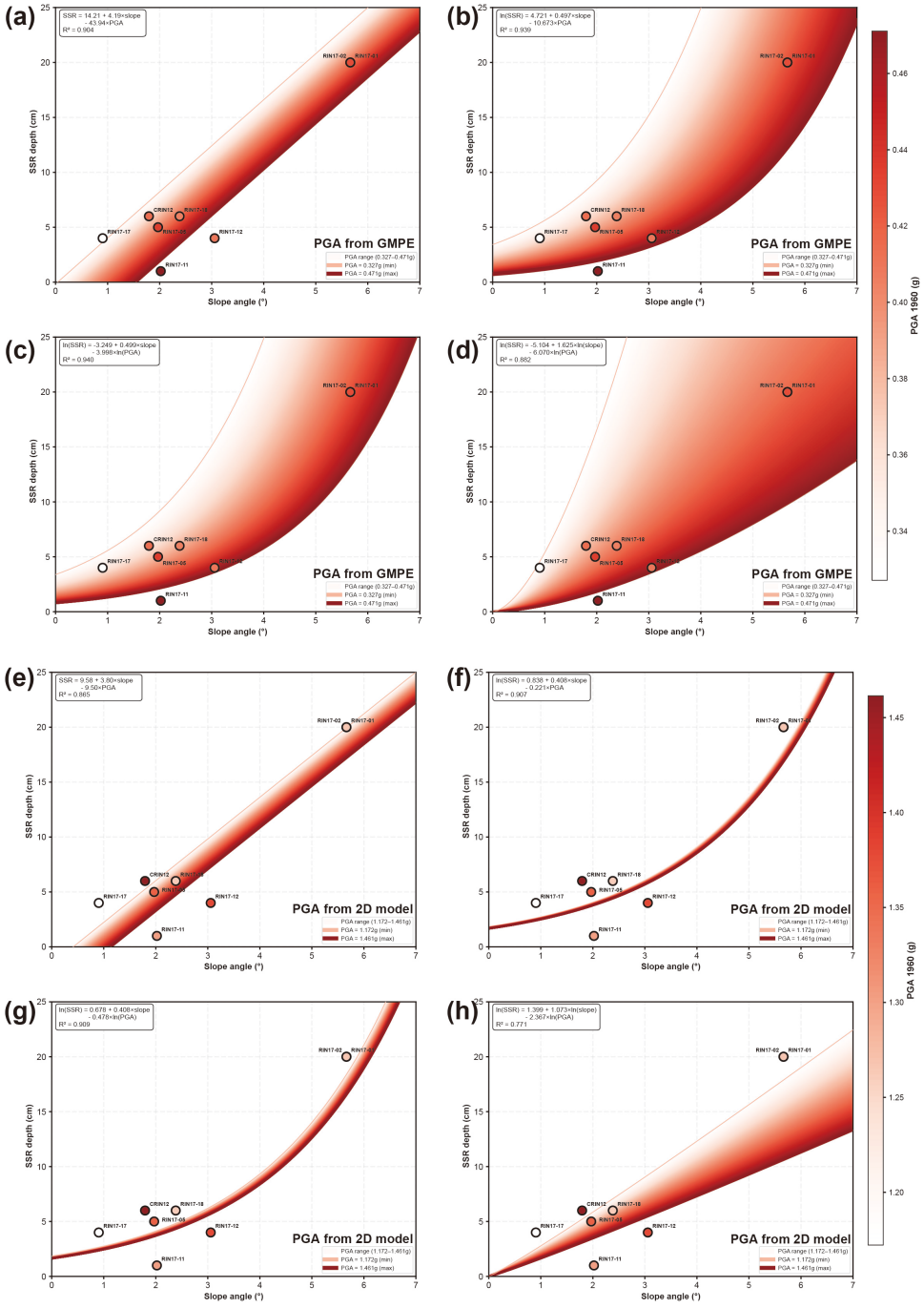

Figure S9. Multivariate regressions of SSR depth against slope angle and PGA for the 1960 Mw 9.5 Valdivia earthquake. (a–d) PGA from GMPE predictions; (e–h) PGA from 2D simulations. Four regressions are tested for each data source (Table S3). PGA is projected as red shading. Regression equations and R^2 values are in each figure. Labeled circles indicate to core sites.

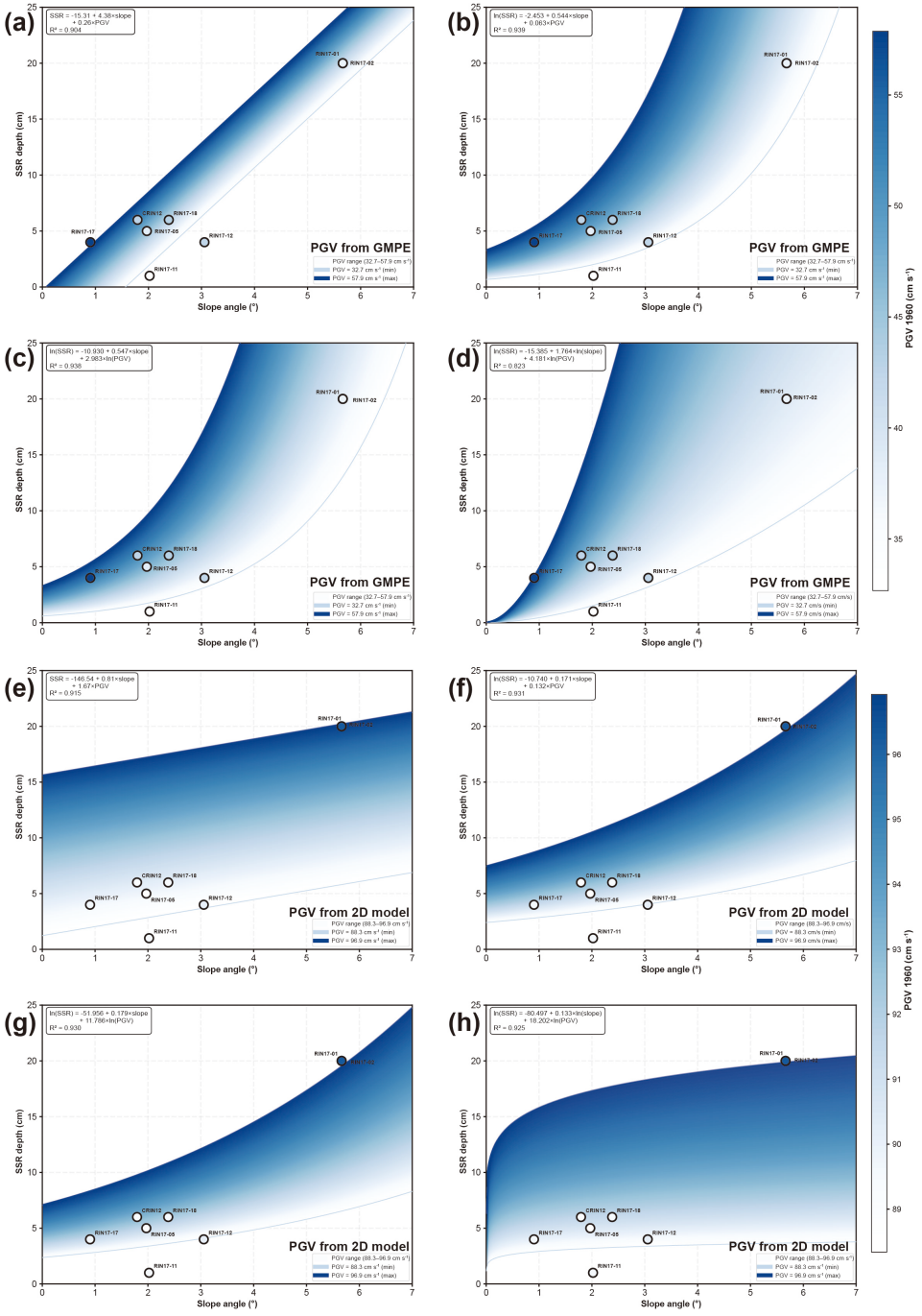

Figure S10. Multivariate regressions of SSR depth against slope angle and PGV for the 1960 Mw 9.5 Valdivia earthquake. (a–d) PGV from GMPE predictions; (e–h) PGV from 2D simulations. Four regressions are tested for each data source (Table S3). PGV is projected as blue shading. Regression equations and R^2 values are in each figure. Labeled circles indicate to core sites.

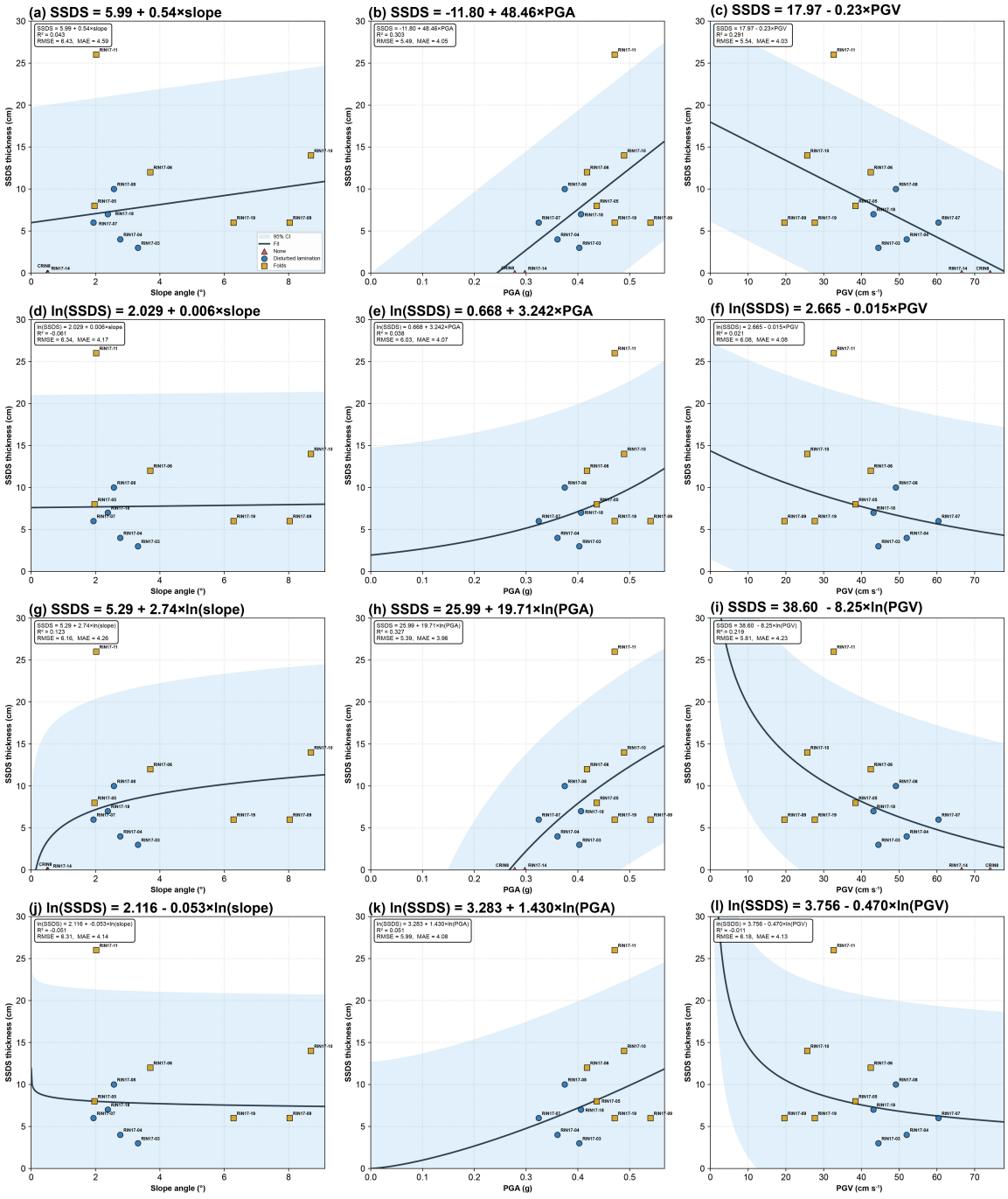

Figure S11. Univariate regressions of SSDS thickness with slope angle, PGA, and PGV (from GMPE predictions) for the 1960 M_w 9.5 Valdivia earthquake, testing four regressions (Table S3). Each column represents a different predictor: slope angle (a, d, g, j), PGA (b, e, h, k), and PGV (c, f, i, l). Regression equations, R^2, RMSE, and MAE values are in each figure. Solid lines show best-fit regressions with 95% confidence intervals (shaded). Symbols distinguish SSDS types as none, disturbed laminations, and folds. PGA has the highest R^2 among all single predictors (h), while PGV coefficients are negative across all regressions.

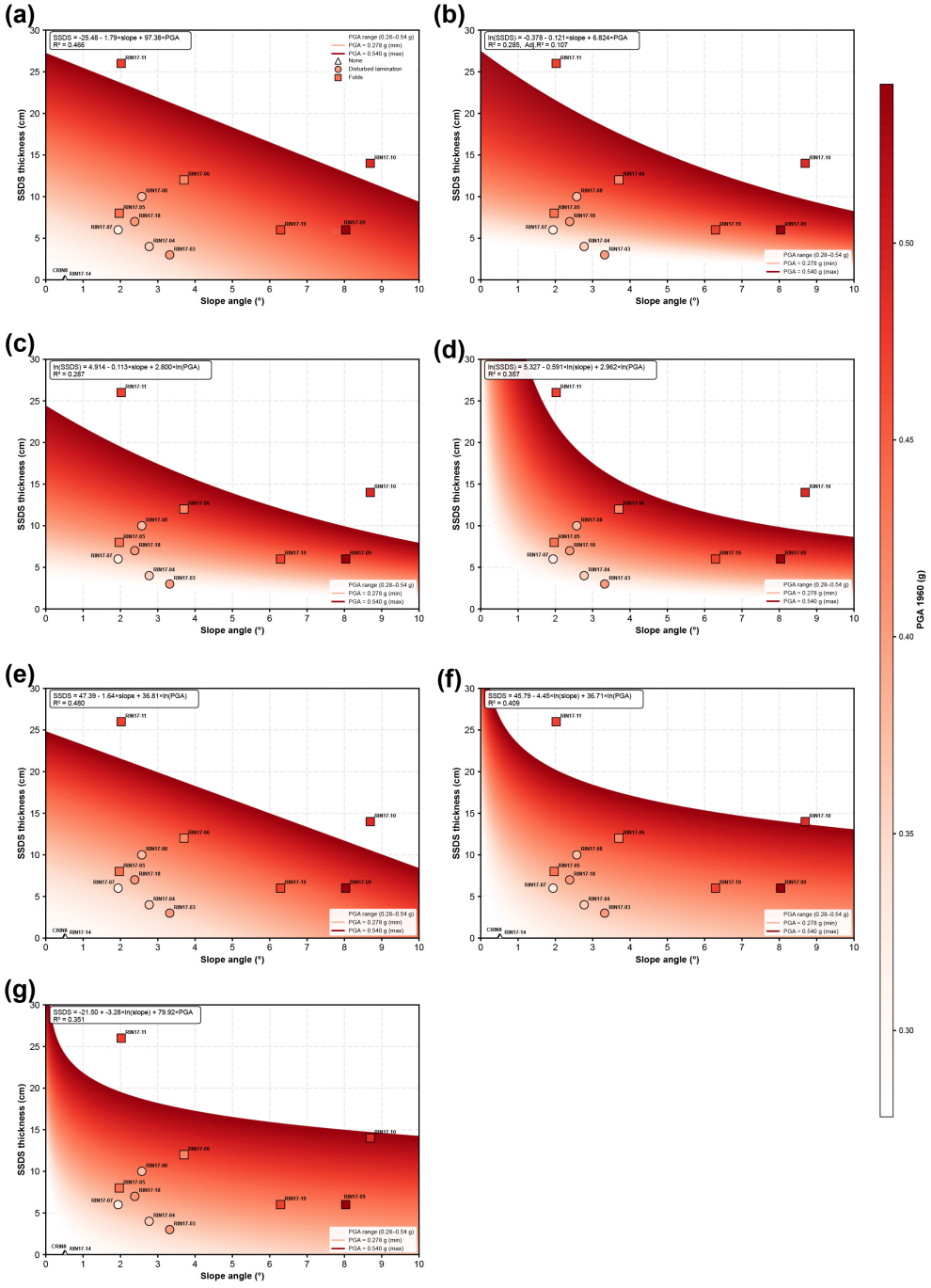

Figure S12. Multivariate regressions of SSDS thickness with slope angle and PGA (from GMPE predictions) for the 1960 M_w 9.5 Valdivia earthquake, testing seven regressions (Table S3). Regression equations and R^2 values are in each figure. Symbols distinguish SSDS types as none (circles), disturbed laminations (pentagons), and folds (squares). PGA is projected as red shading. The highest R^2 (0.48) is obtained in (e), with positive PGA coefficients across all regressions.

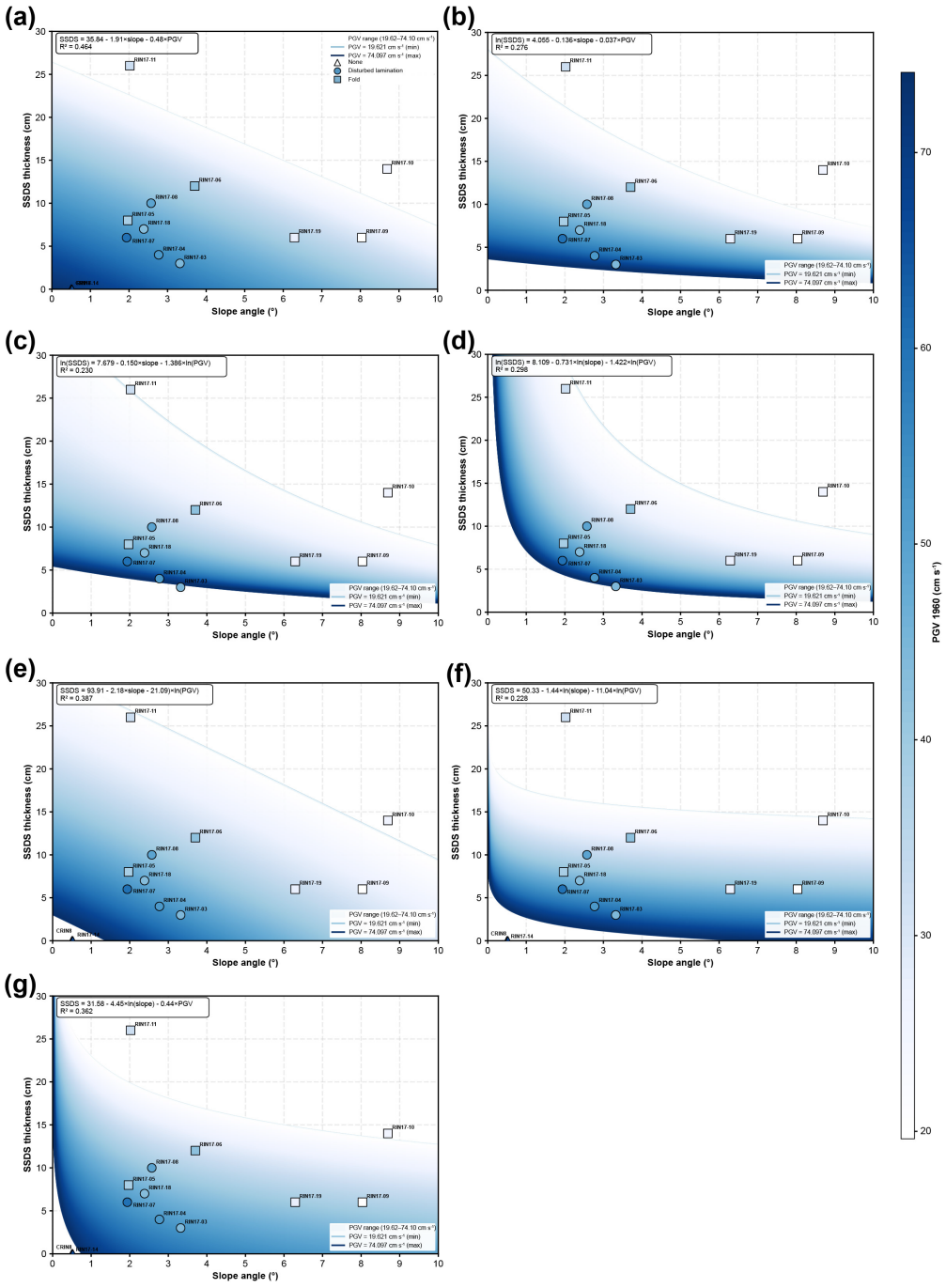

Figure S13. Multivariate regressions of SSDS thickness against slope angle and PGV (from GMPE predictions) for the 1960 Mw 9.5 Valdivia earthquake, testing seven regressions (Table S3). Regression equations and R^2 values are in each figure. Symbols distinguish SSDS types as none (triangles), disturbed laminations (circles), and folds (squares). PGV is projected as blue shading.. All regressions yield negative PGV coefficients and lower R^2 values (≤0.36).

Table S1. Key parameters for the 2D numerical modeling with unconsolidated glaciolacustrine deposits.

Layer	Geological stratum	Bulk density (g cm^{-3})	V_p (m s^{-1})	V_s (m s^{-1})	Shear modulus (Pa)	Bulk modulus (Pa)	Friction Angle (°)
Unit 3	Holocene sediments	1.2	1450	100	1.21×10^{7}	2.42×10^{9}	33
Unit 2	Glaciolacustrine deposits	1.6	1800	200	640×10^{7}	5.10×10^{9}	36
Unit 1	Glacial till	2.3	2400	400	3.68×10^{8}	1.18×10^{10}	40
Unit 0	Basement	2.6	3000	1000	2.60×10^{9}	1.95×10^{10}	45

Table S2. Detailed material properties for each stratigraphic unit in the seven basin model.

Model	Unit	ρ (g cm^{-3})	G (Pa)	K (Pa)	c (Pa)	φ (°)
Basin Model 01	3	1.2	1.21×10^7	2.42×10^9	2000	33
	2	1.6	6.23×10^7	7.45×10^9	10000	36
	1	2.3	3.68×10^8	1.18×10^{10}	20000	40
	0	2.6	2.60×10^9	1.95×10^{10}	100000	45
Basin Model 02	3	1.2	1.21×10^7	2.42×10^9	2000	33
	2	1.6	6.23×10^7	7.45×10^9	10000	36
	1	2.6	2.60×10^9	1.95×10^{10}	100000	45
	0	2.6	2.60×10^9	1.95×10^{10}	100000	45
Basin Model 03	3	1.2	1.21×10^7	2.42×10^9	2000	33
	2	2.6	2.60×10^9	1.95×10^{10}	100000	45
	1	2.6	2.60×10^9	1.95×10^{10}	100000	45
	0	2.6	2.60×10^9	1.95×10^{10}	100000	45
Basin Model 04	3	1.6	6.23×10^7	7.45×10^9	10000	36
	2	1.6	6.23×10^7	7.45×10^9	10000	36
	1	2.3	3.68×10^8	1.18×10^{10}	20000	40
	0	2.6	2.60×10^9	1.95×10^{10}	100000	45
Basin Model 05	3	1.2	1.21×10^7	2.42×10^9	2000	33
	2	1.6	6.23×10^7	7.45×10^9	10000	36
	1	2.3	3.68×10^8	1.18×10^{10}	20000	40
	0	2.3	3.68×10^8	1.18×10^{10}	20000	40
Basin Model 06	3	1.2	1.21×10^7	2.42×10^9	2000	33
	2	1.2	1.21×10^7	2.42×10^9	2000	33
	1	1.2	1.21×10^7	2.42×10^9	2000	33
	0	1.2	1.21×10^7	2.42×10^9	2000	33
Basin Model 07	3	2.6	2.60×10^9	1.95×10^{10}	100000	45
	2	2.6	2.60×10^9	1.95×10^{10}	100000	45
	1	2.6	2.60×10^9	1.95×10^{10}	100000	45
	0	2.6	2.60×10^9	1.95×10^{10}	100000	45

ρ—bulk density, G—shear modulus, K—bulk modulus, c—cohesion, φ—friction angle.

Table S3. Regression results for sedimentary imprint thickness using slope angle and ground motion parameters from GMPE predictions and 2D simulations.

Response Variable	Data Source	Predictor(s)	Equation	R^2	Figure
SSR — Univariate regressions					
SSR	—	Slope	SSR = −2.978 + 3.829×slope	0.850	10
	GMPE	PGA	SSR = −9.96 + 48.77×PGA	0.010	—
	GMPE	PGV	SSR = 26.26 − 0.58×PGV	0.010	—
SSR — Multivariate regressions with PGA (GMPE)					
SSR	GMPE	Slope + PGA	SSR = 14.21 + 4.19×slope − 43.94×PGA	0.904	S9a
	GMPE	Slope + PGA	ln(SSR) = 4.721 + 0.457×slope − 10.673×PGA	0.939	S9b
	GMPE	Slope + ln(PGA)	ln(SSR) = −3.249 + 0.409×slope − 3.998×ln(PGA)	0.940	S9c
	GMPE	ln(Slope) + ln(PGA)	ln(SSR) = −5.104 + 1.625×ln(slope) − 6.070×ln(PGA)	0.882	S9d
SSR — Multivariate regressions with PGA (2D model)					
SSR	2D model	Slope + PGA	SSR = 9.58 + 3.80×slope − 9.50×PGA	0.805	S9e
	2D model	Slope + PGA	ln(SSR) = 0.838 + 0.408×slope − 0.221×PGA	0.907	S9f
	2D model	Slope + ln(PGA)	ln(SSR) = 0.678 + 0.408×slope − 0.478×ln(PGA)	0.909	S9g
	2D model	ln(Slope) + ln(PGA)	ln(SSR) = 1.399 + 1.073×ln(slope) − 2.367×ln(PGA)	0.771	S9h
SSR — Multivariate regressions with PGV (GMPE)					
SSR	GMPE	Slope + PGV	SSR = −15.31 + 4.38×slope + 0.26×PGV	0.904	S10a
	GMPE	Slope + PGV	ln(SSR) = −2.455 + 0.544×slope + 0.063×PGV	0.939	S10b
	GMPE	Slope + ln(PGV)	ln(SSR) = −10.930 + 0.547×slope + 2.863×ln(PGV)	0.938	S10c
	GMPE	ln(Slope) + ln(PGV)	ln(SSR) = −15.385 + 1.764×ln(slope) + 4.181×ln(PGV)	0.823	S10d

SSR — Multivariate regressions with PGV (2D model)					
SSR	2D model	Slope + PGV	SSR = −146.54 + 0.81×slope + 1.67×PGV	0.915	S10e
	2D model	Slope + PGV	ln(SSR) = −10.740 + 0.171×slope + 0.132×PGV	0.931	S10f
	2D model	Slope + ln(PGV)	ln(SSR) = −51.956 + 0.179×slope + 11.788×ln(PGV)	0.930	S10g
	2D model	ln(Slope) + ln(PGV)	ln(SSR) = −80.497 + 0.133×ln(slope) + 18.202×ln(PGV)	0.925	S10h
SSDS — Univariate regressions (GMPE)					
SSDS	—	Slope	SSDS = 5.99 + 0.54×slope	0.043	S11a
	GMPE	PGA	SSDS = −11.80 + 48.46×PGA	0.303	S11b
	GMPE	PGV	SSDS = 25.90 − 0.56×PGV	0.252	S11c
	—	Slope	ln(SSDS) = 2.029 + 0.006×slope	0.061	S11d
	GMPE	PGA	ln(SSDS) = 0.668 + 3.242×PGA	0.038	S11e
	GMPE	PGV	ln(SSDS) = 3.067 − 0.033×PGV	0.005	S11f
	—	Slope	SSDS = 5.29 + 2.74×ln(slope)	0.123	S11g
	GMPE	PGA	SSDS = 25.99 + 19.71×ln(PGA)	0.327	S11h
	GMPE	PGV	SSDS = 61.23 − 15.46×ln(PGV)	0.203	S11i
	—	Slope	ln(SSDS) = 2.116 − 0.053×ln(slope)	0.051	S11j
	GMPE	PGA	ln(SSDS) = 3.283 + 1.430×ln(PGA)	0.051	S11k
	GMPE	PGV	ln(SSDS) = 4.796 − 0.806×ln(PGV)	0.024	S11l

SSDS — Multivariate regressions with PGA (GMPE)					
SSDS	GMPE	Slope + PGA	SSDS = −25.48 − 1.79×slope + 97.38×PGA	0.466	S12a
	GMPE	Slope + PGA	ln(SSDS) = −0.378 − 0.121×slope + 6.824×PGA	0.285	S12b
	GMPE	Slope + ln(PGA)	ln(SSDS) = 4.914 − 0.113×slope + 2.800×ln(PGA)	0.287	S12c
	GMPE	ln(Slope) + ln(PGA)	ln(SSDS) = 5.327 − 0.591×ln(slope) + 2.962×ln(PGA)	0.357	S12d
	GMPE	Slope + ln(PGA)	SSDS = 47.39 − 1.64×slope + 36.81×ln(PGA)	0.480	S12e
	GMPE	ln(Slope) + ln(PGA)	SSDS = 45.79 − 4.45×ln(slope) + 36.71×ln(PGA)	0.409	S12f
	GMPE	ln(Slope) + PGA	SSDS = −21.50 − 3.28×ln(slope) + 79.92×PGA	0.351	S12g
SSDS — Multivariate regressions with PGV (GMPE)					
SSDS	GMPE	Slope + PGV	SSDS = 35.84 − 1.91×slope − 0.48×PGV	0.464	S13a
	GMPE	Slope + PGV	ln(SSDS) = 4.055 − 0.136×slope − 0.037×PGV	0.276	S13b
	GMPE	Slope + ln(PGV)	ln(SSDS) = 7.679 − 0.150×slope − 1.386×ln(PGV)	0.230	S13c
	GMPE	ln(Slope) + ln(PGV)	ln(SSDS) = 8.109 − 0.731×ln(slope) − 1.422×ln(PGV)	0.298	S13d
	GMPE	Slope + ln(PGV)	SSDS = 93.91 − 2.18×slope − 21.09×ln(PGV)	0.387	S13e
	GMPE	ln(Slope) + ln(PGV)	SSDS = 50.33 − 1.44×ln(slope) − 11.04×ln(PGV)	0.228	S13f
	GMPE	ln(Slope) + PGV	SSDS = 31.58 − 4.45×ln(slope) − 0.44×PGV	0.362	S13g